WATER TRANSPORT PROPERTIES OF CEMENT MORTARS WITH MUSSEL SHELL AGGREGATE

Martínez-García, Carolina[1]; González-Fonteboa, Belén[1*]; Carro-López, Diego[1]; Martínez-Abella, Fernando[1]

[1]School of Civil Engineering. Department of Construction Technology, University of A Coruña. Postal Address: E.T.S.I. Caminos, Canales, Puertos. Campus Elviña s/n, 15071 La Coruña, Spain.

*Corresponding author; e-mail: bfonteboa@udc.es

Abstract

Aquaculture and cannery industry are important economic sectors in different countries. It generates big profits and create thousands of employment. However, it also produces lots of waste, being bivalve shells remarkable because of their volume. Shell residue usually is disposed in dump sites producing a great environmental impact. Nevertheless, some research works have proved that it is possible to reuse shells in several industrial activities, including construction.

In general, cementitious pastes are commonly used in construction so that the use of aggregates with less environmental impact can be a way to reduce the carbon footprint associated with construction.

Thus, this study aims to analyse the effect of replacing natural aggregate by heat-treated, crushed and sieved mussel shell in cement mortars for coating. An MC 12.5-X (without air entraining agent) was used for cement mortars, with three substitution percentages of limestone aggregate with mussel shell aggregate: 25%, 50% and 75%. The results were compared with those obtained with a reference mortar without mussel shell aggregate. Different tests of water transfer properties have been studied: capillary uptake, water absorption, water vapour permeability and water permeability. The elongated shape of mussel shell and the presence of organic compounds (polysaccharides), lead mussel shells aggregate to disturb the water transfer properties of cement mortars. Results show that mussel shell mortars hinder water capillary uptake, increase the water absorption and both water and water vapour permeability.

Keywords:

Mussel shell, coating cement mortars, capillarity, water absorption, water vapor permeability, water permeability

1 INTRODUCTION

Aquaculture and cannery industry are important economic sectors in Galicia. They generate big profits and create thousands of employment. However, they also produce loads of waste, in which mussel shells are remarkable because of their volume. Galicia generates around 25,000t of mussel shell residue every year that usually are disposed in dump sites producing a great environmental impact.

On the other hand, sand is one of the most used natural resources in the world being construction sector its main consumer. The global aggregates production exceeds 50bnt (billions metric tons) every year. In some countries the aggregates used to mortar and concrete production have been obtained from quarries producing an obvious environmental impact, destroying natural habitats and transforming the landscape. In addition, the aggregate production process developed in quarry plants involves extraction, crushing, grinding and screening and, undoubtedly leads to a high energy consumption and contributes to CO_2 emissions.

According to the final estimations of the Spanish association ANEFA, in 2017 construction sector has ended up with a total consumption of natural aggregates of 112 million tons. An important volume of these aggregates (58%) is consumed in the mortar, concrete and precast industry. For this reason, this study attempts to incorporate mussel aggregates (a by-product from the canning industry) in this field.

Actually, different publications dealing with the feasibility of using seashells in mortar or concrete fabrication have increased in the last 10 years. Some of these works incorporate the seashells as aggregates in concrete [(Halim et al., 2018; Lejano, 2017; Mo et al., 2018, 2016], other authors produce filler from the seashells and use it as a substitute of the cement [Ballester et al., 2007; Mohammad et al., 2017]. One recent work demonstrates the feasibility of using mussel shell as a source of calcium carbonate to synthesize belite rich cement by a heat solid state activation [Bouregba, A. et al., 2018]. There are also some studies that analyse the incorporation of oyster shells [Wang et al., 2013; Yoon et al., 2003; Yoon, 2004] or cockle shells or a mix of seashells as aggregate in different kind of mortars [Liang and Wang, 2013; Motamedi et al., 2015; Nazari and Ghafouri Safarnejad, 2013]. Finally, a work was found that incorporates seashells in cement mortars for masonry and plastering [Lertwattanaruk et al., 2012].

As stated in the literature, mussel shell is composed mainly by calcium carbonate and organic matter content that is located inside its microstructure (chitin). It is well known that the organic matter causes different effects in cement mortar properties. Some authors [Kochova et al., 2017] registered that organic matter can act as a retarder in cement mortars, increasing the workable life time. Other works show that the effect of the organic matter is similar to that air entraining agents have in cement mixes, introducing air voids in cement paste.

Thus, this study aims to analyse the effect of replacing conventional aggregate by mussel shell in mortar fabrication. Mussel shell used are Galician farmed ones, that after a heat treatment are converted into a by-product ready to be used as an aggregate. Mixes were designed in order to create two different coatings: a base and a surface layer coating. Baseline coatings with conventional sand were compared to mussel shell mortars made using different substitution rates (25%, 50% and 75% by volume). Different fresh state properties were studied and, at hardened state, microstructure and pore size distribution were analysed to further understand hardened behaviour.

2 MATERIALS AND MIXES

2.1 Cement and aggregate

The cement used was a masonry cement MC12.5-X (without air entraining agent). The cement composition is: portland cement (clinker 41.3%) and inorganic compounds (limestone 33.5%, calcined natural pozzolana 19.8%, gypsum 5.4%). Results of the X-ray diffraction (XRD) characterisation are shown in Tab. 11.

Tab. 11: Chemical composition by XRD characterisation of MC12.5-X.

	%
CaO	48.5
SiO_2	17.9
Al_2O_3	6.1
Fe_2O_3	3.7
SO_3	3.5
MgO	1.5
K_2O	1.1
Na_2O	0.55
TiO_2	0.28
P_2O_5	0.069
SrO	0.064
ZnO	0.048
Cl	0.046
MnO	0.040
ZrO_2	0.034
CuO	0.022
LOI 550ºC	2.9
LOI 975ºC	16.5

The sand used comes from a crushed limestone with a maximum size of 4 mm. From this sand, two different fractions were obtain by sieving. A fine sand (0-1mm-FNS) and a coarse sand that was obtained combining different fractions of the original limestone sand (0-4 mm-NS) (Fig. 1). The sieve modulus of the NS was 2.23.

Fig. 1: Sand aggregates: a) Limestone sand 0-0.063mm b) Limestone sand 0.063-0.25 mm c) Limestone sand 0.25-1mm d) Limestone sand 1-4mm e) Fine mussel shell sand (FMS) 0-1mm f) Coarse mussel shell sand (CMS) 0-4mm.

Mussel shell supplied was heat-treated according to European regulation (European Parliament and Council, 2009) (135°C for 32 minutes). X-ray diffraction (XRD) characterization of mussel shell shows that it is composed mainly of calcium carbonate (95%), and is formed by the bio-mineralisation of CaCO3 with a small amount of organic matrix which holds the structure together, as was shown in a previous work [Martínez-García et al., 2017].

Two mussel shell sands, a coarse sand (0-4mm-CMS) and a fine sand (0-1mm-FMS) were supplied after a grinding and sieving process of the heat-treated mussel shell. Finally the mussel shell sand (0-4mm-MS) used, was obtained from the mixture of the two supplied fractions with an equivalent particle size distribution to the natural one (NS). The mix percentages used were 88.5% of FMS and 11.5% of CMS (Fig. 2). The resulting sieve modulus of MS was 2.21.

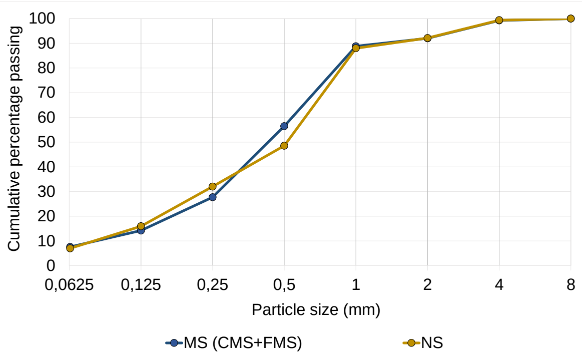

Fig. 92: Particle size distribution of aggregates used.

The particle density, measured according UNE-EN 1097-6 of different aggregate were 2.72 kg/dm3 for MS, and 2.67kg/dm3 for NS. Sand equivalent (UNE-EN 933-8) measured for mussel shell sand was 71.77% and for natural sand was 64%. The water absorption, measured according UNE-EN 1097-6, of the aggregates were 3.94% for the mussel sand and for the natural sand 2.22%. Chlorides content (UNE-EN 1744-1) of the mussel shell sand was 0.48%. Soluble sulfates content for the mussel shell sand was 0.59% and total sulfates was 1.33% (both according to UNE-EN 1744-1). Organic matter content of mussel shell sand was 2.07% for de mussel shell sand, measured according to UNE 103204:93.

2.2 Mix design

Baseline mix of cement coating (CC) mortar was designed. Mix proportions were chosen to ensure high enough workability so that high percentages of mussel shell sand could be incorporated.

The mortar dosage was designed with a cement:sand ratio of 1:5 (by volume) and a water:cement ratio of 1 (by weight).

Mussel mortars were designed replacing conventional sand by mussel shell sand by volume. The replacing percentages used were 25%, 50% and 75%. So four mussel shell cement mortars were obtained: CC0, CC25, CC50 and CC75. Tab.2 shows the mix proportions of the reference mortars and of the mussel shell mortars.

Tab. 12: Baseline and mussel shell mortars dosage (g per litre).

	Substitution rate (%)			
	0	25	50	75
Cement	312.02			
Water	312.02			
NS	1560.12	1170.09	780.06	390.03
MS	0	397.33	794.67	1192.00

3 TEST METHODS

3.1 Mixing and moulding

The raw materials were mixed in order to obtain the different mortars. The mixing procedure was developed according to UNE-EN 196-1: firstly, cement and water were blended for 30 seconds at low speed. Then the aggregate was added and mixed for 30 seconds at low speed and 30 seconds at high speed. The mixing procedure was then stopped for 90 seconds, the mixer walls were scrapped in the first 30 seconds and finally, mixing continued for 60 seconds at high speed. Different batches were made to determine hardened state behaviour of each mortar.

In order to develop hardened state tests, mortars were cast in different moulds and were maintained in the moulds for 2 days before demoulding. All mortars were cured in a climatic chamber and both the temperature and relative humidity were fixed at 20 °C ± 2 and 60 ± 5%, respectively.

3.2 Microstructure

At the age of 3 and 28 days, different mortar samples were pre-consolidated by impregnation with resin under vacuum. Thin slices were cut to a thickness of approximately 20 microns. Then the samples were polished, covered with a glass slip and examined with LEICA DM750M optical microscopy. Specimens used for scanning electron microscopy (SEM) were dehydrated and covered with gold in a Bal-Tec SCD 004 sputter coater. In addition, some samples were examined and photographed using a JEOL JSM-6400 Scanning Electron Microscope.

3.3 Porosity, pore size distribution and water absorption

Porosity accessible for water were measured according to UNE 83980 at 28 days. For this test, circular moulds with a diameter of 150mm and a thickness of 20 mm were used. By means of a core-drill, at least three pieces of each mortar were taken from different samples of hardened cement mortars at the age of 28 days for measure water absorption and porosity accessible to water. The samples were saturated under water during 24-48hs until stable mass was measured. After that, samples were boiling during 5 hours. The test pieces are allowed to cool in water for at least 15 hours. The next day they samples are weighed on a hydrostatic scale. Density, water absorption and porosity after immersion and after boiling were calculated.

Other little pieces (2 to 3 g) of hardened samples at 28 days age were used to measure the pore size distribution with a Mercury Intrusion Porosimetry (MIP). This test was performed using a Poremaster-60 GT mercury porosimeter, which automatically registers pressure (between 6.29 KPa to 410759.65 KPa), pore diameter in a range between 0.003 to 200 µm, intrusion volume, and pore surface area.

3.4 Water absorption by capillarity

The water absorption by capillarity test was determined according to UNE EN 1015-18 at 28 days. Three 160x40x40 mm samples of each mortar were used for this test. After drying them to constant mass, the four largest faces of the specimens were sealed using paraffin, and then they were broken into two halves. Test pieces (six samples of each mortar) were placed on a tray with the broken face turned down on four supports so that they did not touch the bottom of the tray. The samples were maintained immersed in water to a height of 5 to 10 mm from their bottom. The specimens were weighed at two intervals (10 and 90 min) and the weight gain due to capillary absorption was recorded. Data were used to plot a graph showing the weight gain per unit of specimen base area versus the square root of time. The slope of the line is the capillary absorption coefficient.

3.5 Water vapour permeability

Water vapour permeability test was carried out according to UNE EN 1015-19 at 28 days. Testing samples were made in a cylindrical PVC mould of 150 mm diameter and 18 mm height based on a cellular concrete support covered with a gauze. The samples were maintained in the climatic chamber until the testing age. Just before the test, mortar samples were introduced in a circular stainless steel plate of 150 mm diameter. A fixed volume of a potassium nitrate solution was placed at the bottom of the plate to provide a high indoor humidity (> 90%). The volume was fixed so that the samples were separated from the solution approximately 1cm. The union between the steel mould and the specimen was sealed with petroleum jelly (Fig. 3). The sealed samples were placed in the climatic chamber at 20°C and 60% of relative humidity during the testing measurements. Samples were weighed every day until water vapour transfer is stable (that is when three consecutive measurements are on a straight line).

Fig. 93: Water vapour permeability test.

3.6 Water permeability

The water permeability test was carried out as follows: specimens manufactured in the same way as those used for the water vapour permeability test were cured for 28 days. Then a plastic cone with a height of 100 mm and a base-diameter of 80 mm was placed on the sample top face (Fig.4). The perimeter of the cone and the rest of the test specimen (its top face and its edge) were sealed with paraffin. Afterwards, samples were placed on a metal grill. Then the cone was filled with water and a bottle provides the required water to maintain the cone filled for 48 hours.

Fig. 94: Water permeability test.

4 RESULTS AND DISCUSSION

4.1 Microstructure

Fig. 4 show SEM images of baseline mortar (CC0) and mussel shell mortars with 75% replacement percentage (CC75).

At three days age, the images show a microstructure with lower porosity in both baseline mortar (Fig. 4a) than in mussel shell mortar. The structure of CC75 presents small and numerous pores, showing a microstructure similar to that formed when air entrainment additives are used [Mendes et al., 2017; Topçu et al., 2017]. These air entrained pores are rounded voids formed by the organic compounds present in the shell structure. Different authors [Dalbeck et al., 2006; Dauphin et al., 2003] suggest that sulphated compounds and S-containing amino acids are associated with intercrystalline structures and intracrystalline organic matrix of mollusc shells.

Micrographs also show smooth areas with elongated and concave shape in the cement paste of mussel shell mortars. It is likely that these areas correspond to the region of cement paste around the shell particles, denoting a poor paste-aggregate bond when these aggregates are used. In addition, this contact area also presents high porosity, confirming, again, that mussel shell aggregate produces high cement paste voids.

At 28 days age, in Fig. 5 c (corresponding to CC75) the interfacial transition zone (ITZ) between the cement paste and a large size mussel shell particle can be seen. The image confirms that there is a significant lack of bond between the shell particle and the cement matrix, and shows an ITZ with a significant crack width. In addition, many cracks can be seen throughout the mussel particle and throughout the cement paste.

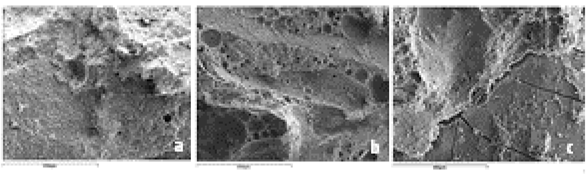

Fig.95: SEM images (100x) of cement mortars: a)CC0 at 3 days, b) CC75 at 3 days, c) CC75 at 28 days.

Optical microscopy photographs were used to measure pores larger than 200 microns that are not detected with mercury porosimetry (Fig. 6). Fig. 6 shows large pores (above 500 μm) in mortar with a substitution rates of 75%. Moreover, sometimes, these pores get to connect different mussel aggregates.

In addition, cement paste surrounding mussel shell sand presents lots of small round pores, like those generated by entrapped air during mixing, although they present irregular distribution into the paste.

All these results lead to conclude that mussel shell increases mortar porosity considerably. In addition to the air volume generated, it has to be taken into account that this porosity creates countless of ITZ between pores and paste that will also affect mortar properties. Fig. 6b shows the ITZ generated in a large air void of CC75 coatings. Most of the large air voids are going to present a similar structure. Other authors [Rashed and Williamson, 1991] state that air voids due to air entrainment present two distinct features: a shell to the air void surface and an interfacial transition zone between this shell and the bulk cement paste. Moreover, the paste around the voids has higher water content than the paste farther away from the interface. According to Piasta and Sikora [Piasta and Sikora, 2015], interfacial paste of porous microstructure occupies a large part of cement paste volume. The air void interfaces can even overlap and interconnect. Therefore, mussel shell aggregate generate countless of these porous ITZ that, doubtless, will affect mortar properties.

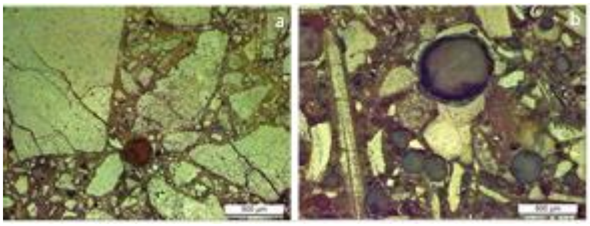

Figure 96: Optical microscopy images of cement coatings: a) CC0, b) CC75.

4.2 Pore size distribution, porosity and water absorption

Pore size distribution of the different mortars is shown in Fig. 7. It can be seen that the incorporation of mussel shell sand modifies the pore size distribution of the mortars. This is notably when the replacement ratio of conventional sand by mussel shell sand is higher than 25%. Up to 25%, mussel shell mortars present a pore size distribution that, although shows a high volume of large pores, is slightly similar to the pore distribution of the reference mortars. However, when 50% and 75% substitution rates are used, the pore size distribution of mussel mortars is considerably different from the distribution of the baseline mortars.

The analysis of the curves leads to state that the incorporation of mussel shell aggregate significantly increases the pore volume and generates many pores with high diameter. In this regard, all curves move towards the right side of the graph. This indicates that the pore volume of large size pores (in the range of 1 to 100 μm) significantly increases while the pore volume of small size pores (in the range of 0.01 to 0.3 μm) slightly decreases (50% and 75% replacement ratios) or it is maintained (25% replacement rate).

This pore size distribution is in agreement with micostructure. It is clear that the use mussel shell as sand aggregate leads to higher cement matrix porosity. The irregular shape of the particles and the presence of chitin in mussel composition introduce large pores and damage the ITZ reducing the bond between the binder and the mussel aggregate (which is also related to the presence of large pores in the matrix.

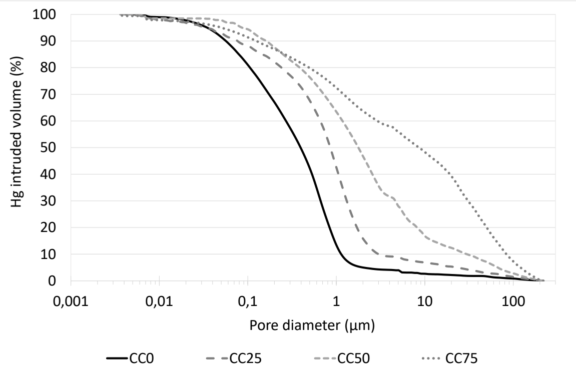

Fig. 97: Pore size distribution of cement coatings.

Fig. 8 shows porosity accessible to water after immersion, after immersion and boiling and porosity measured by mercury intrusion. In agreement with previous results, porosity is higher in mussel mortars than in baseline mortars. In addition, results show that porosity values of all cement mortars are higher after water boiling than after water immersion, being the difference more noticeable in mussel shell mortars than in baseline mortars. This highlights that air bubbles (that may not be well communicated) are part of the porous structure of mussel mortars. It is when boiling the samples that most of the total open porosity is filled with water.

In this work, results show that when substitution rates of 50% and 75% are used, the boiling water porosity is higher than the MIP porosity. The high volume of large pores (>500µm), that are not being measured with MIP, justify this results.

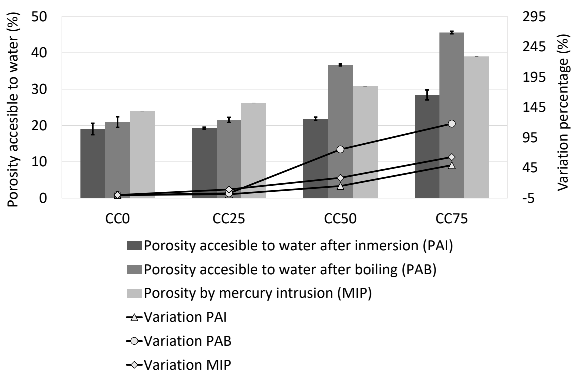

Fig. 98: Prosity of cement coatings.

Fig. 9 shows water absorption at 28 days. These water absorption values are directly related to open porosity. Therefore, as happens with porosity, water absorption is higher in mussel mortars than in baseline mortar. In addition, water absorption after boiling is higher than after immersion.

Finally, in agreement with other results developed in this work and found in the literature [Safi et al., 2015], the use of high replacement percentages (50% and 75%) significantly affect this property, however, when only 25% replacement rate is used, water absorption of mussel mortars is only slightly higher than hat measured in baseline coatings. Air entrainment or entrapment produced by mussel shell organic matter content and its flaky particle shape and the low bond between mussel shell and cement paste generate large pores that lead to increase mussel coating water absorption.

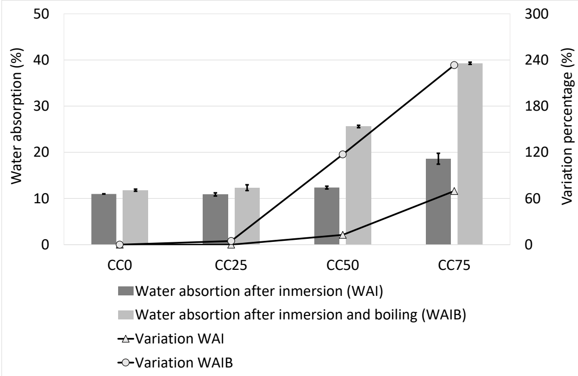

Fig 99: Water aborption of cement coatings.

4.3 Water absorption by capillarity

Fig. 10 shows the water absorption due to capillary action measured at 28 days between 10 and 90 minutes. The results indicate that mussel shell aggregate decreases the capillary uptake of cement mortars. The reductions are of about 40% when the 25% of mussel aggregate is used and almost 70% in CC75.

According to the requirements established in UNE-EN 998-1 for capillary absorption in rendering mortars, all mortars (but CC75) can be classified as W0. Anyway, mortars with 75% of mussel aggregate can be classified as W1 (≤0.40 $kg/m^2min^{0.5}$), which allows them to be used as thermal insulation coatings.

The water absorption due to capillary action depends, not only on the total mortar porosity, but also on mortars' pore size distribution [Silva et al., 2016]. As seen in section 5.2., capillary pores (micropores and the small mesopores pores) are lower in mussel shell coatings than in baseline coatings, being the volume of large pores (>500µm) higher in the former than in the latter. This issue, joined to the particle shape of mussel shells (elongated and with large smooth surface areas) act as a barrier to capillary water ascension. No works were found about capillarity in seashell cement mortars.

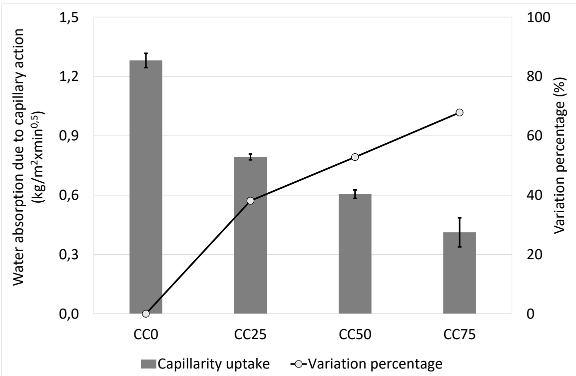

Fig. 100: Water absortion by capillarity of cement coatings.

4.4 Water vapour permeability

Fig. 11 shows the results of the water vapour permeability of cement coatings. The use of mussel shell significantly increases the water vapour permeability of coatings. These values indicate that water vapour permeability is a 250% higher in CC25 than in CC0. This increment is about 350% when CC75 is analysed.

The mussel shell creates a more porous system in the cement mortar matrix that facilitates the water vapour diffusion process through the structure.

The porous system of mussel shell coatings and the existence of channels facilitates the water vapour diffusion process through the structure [Fernandes et al., 2005].

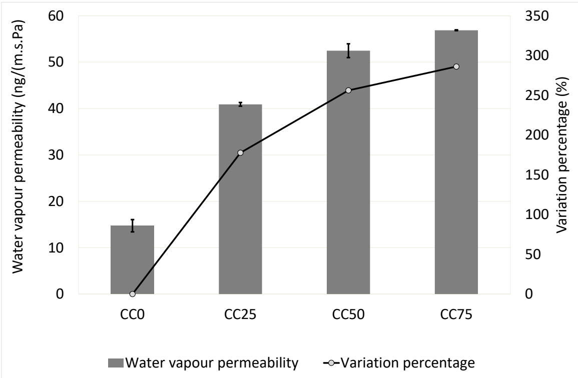

Fig. 101: Water vapour permeability of cement coatings.

4.5 Water permeability

Water permeability results are shown in Fig. 12. In this case, BC0 and BC25 present similar water permeability values, differences do not exceed 18%. BC50 results at first 2 hours varies in nearly a 13% and reaches nearly the 75% at 48 hours from the reference sample values. In the test of BC75 sample all, the water permeated through the sample in the first 30 minutes. Thus, variations from BC0 results are above the 90%.

This behaviour of the BC75 mortar could be assimilated to that of a pervious material, although the recommended values for water permeability of pervious concrete are somewhat higher (0.2-5.4 mm/s). It can be found some works that used different seashells for designing pervious concrete [Nguyen et al., 2017, 2013], so it is possible to think in the feasibility of the mussel shell aggregate for use in pervious concrete. Wong et al. [Wong et al., 2011] stated that the effects of entrained air on microstructure of concretes makes that the porosity near the air void boundary is about 2-3 times that of the bulk paste and that air entrainment increases permeability by up to a factor of 2-3 in case of the highest air contents.

It seems to be clear that these important variations in water permeability are caused again by the change in pore size distribution of mortars due to large pores inserted by mussel shell aggregate.

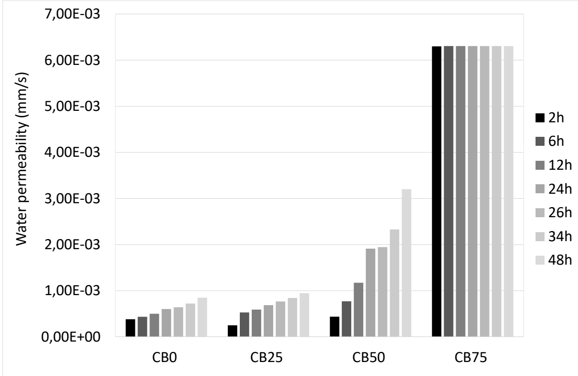

Fig. 102: Water permeability of cement coatings.

5 CONCLUSIONS

This work aimed to investigate the potential use of a by product from the canning industry, mussel shell aggregate, in the production of cement coatings. Cement mortars were designed replacing conventional sand by mussel shell sand. The replacing percentages used were 25%, 50% and 75%, by volume, and the behaviour of the new mixes was compared to the behaviour of the baseline mortar (0%).

Microstructure analysis of cement coatings leads to confirm that the irregular and flaky particles of the mussel sand introduce large pores in cement paste. This means an increase in porosity and water absorption. However, on the contrary, the high volume of large pores (>500µm) joined to the particle shape of mussel shells (elongated and with large smooth surface areas) act as a barrier to capillary water ascension, reducing then, the capillary uptake.

The porous system of mussel shell coating mortars, facilitates the water diffusion process. Large pores inserted by mussel shell particles caused important increases in water permeability.

Further research is needed to study the effect of the mussel shell particles orientation that caused different behaviour of water and vapour flow in mortars.

Finally, form the results obtained with this work, it can be stated that a replacement ratio of 25% of the crushed limestone aggregate by mussel shell aggregate can be used to produce accurate surface and base layer coatings. This joined to the low energy consumption of the heat treatment used to produce the mussel shell aggregate proved that the production of cement coatings with this canning industry by-product is a suitable sustainable solution.

6 ACKNOWLEDGMENTS

This work has been developed within the framework of the project "Valorización de las conchas de bivalvos gallegos en el ámbito de la construcción" (Valorization of Galician bivalve shell in the construction sector; Code 00064742 / ITC-20133094), funded by CDTI (Centro para el Desarrollo Tecnológico e Industrial) under the FEDER-Innterconecta Program, and co-financed with European Union ERDF funds. We wish to express our most sincere thanks to the professionals of the firms Extraco, Serumano and Galaicontrol.

7 REFERENCES

[Ballester et al 2007] Ballester, P., Mármol, I., Morales, J., Sánchez, L., 2007. Use of limestone obtained from waste of the mussel cannery industry for the production of mortars. Cem. Concr. Res. 37, 559–564.

[Bouregba et al 2018] Bouregba, A., Diouri, A., Amor, F., Ez-zaki, H., Sassi, O., 2018. Valorization of glass and shell powders in the synthesis of Belitic clinker. MATEC Web Conf. 149, 1021.

[Dalbeck et al 2006] Dalbeck, P., England, J., Cusack, M., Lee, M., Fallick, A.E., 2006. Crystallography and chemistry of the calcium carbonate polymorph switch in M. edulis shells, European Journal of Mineralogy.

[Dauphin et al 2033] Dauphin, Y., Cuif, J., Doucet, J., Salomé, M., Susini, J., Williams, C., 2003. In situ mapping of growth lines in the calcitic prismatic layers of mollusc shells using X-ray absorption near-edge structure (XANES) spectroscopy at the sulphur K-edge. Mar. Biol. 142, 299–304.

[Fernandes et al 2005] Fernandes, V., Silva, L., Ferreira, V.M., Labrincha, J.A., 2005. Influence of the kneading water content in the behaviour of single-coat mortars. Cem. Concr. Res. 35, 1900–1908.

[Halim et al 2018] Halim, S.D., Rainer, E., Ryantonius, C., Panandito, B., Wardoyo, D., Fahlevy, M.R., Darma, I.S., 2018. The use of hazardous sludge solidification and green-lipped mussel shells in cementitious material: a case study of ngcc power plant of priok. MATEC Web Conf. 147, 01008.

[Kochova et al 2017] Kochova, K., Schollbach, K., Gauvin, F., Brouwers, H.J.H., 2017. Effect of saccharides on the hydration of ordinary Portland cement. Constr. Build. Mater. 150, 268–275.

[Lejano 2017] Lejano, B., 2017. Optimization of compressive strength of concrete with pig-hair fibers as fiber reinforcement and green mussel shells as partial cement substitute. Int. J. GEOMATE 12.

[Lertwattanaruk et al 2012] Lertwattanaruk, P., Makul, N., Siripattarapravat, C., 2012. Utilization of ground waste seashells in cement mortars for masonry and plastering. J. Environ. Manage. 111, 133–141.

[Liang and Wang 2013] Liang, C.F., Wang, H.Y., 2013. Feasibility of pulverized oyster shell as a cementing material. Adv. Mater. Sci. Eng. 2013.

[Martínez-García et al. 2017] Martínez-García, C., González-Fonteboa, B., Martínez-Abella, F., Carro-López, D., 2017. Performance of mussel shell as aggregate in plain concrete. Constr. Build. Mater. 139.

[Mendes et al. 2017] Mendes, J.C., Moro, T.K., Figueiredo, A.S., Silva, K.D. do C., Silva, G.C., Silva, G.J.B., Peixoto, R.A.F., 2017. Mechanical, rheological and morphological analysis of cement-based composites with a new LAS-based air entraining agent. Constr. Build. Mater. 145, 648–661.

[Mo et al. 2018] Mo, K.H., Alengaram, U.J., Jumaat, M.Z., Lee, S.C., Goh, W.I., Yuen, C.W., 2018. Recycling of seashell waste in concrete: A review. Constr. Build. Mater. 162, 751–764.

[Mo et al. 2016]Mo, K.H., Alengaram, U.J., Jumaat, M.Z., Yap, S.P., Lee, S.C., 2016. Green concrete partially comprised of farming waste residues: a review. J. Clean. Prod. 117, 122–138.

[Mohammad et al. 2017] Mohammad, W.A.S.B.W., Othman, N.H., Ibrahim, M.H.W., Rahim, M.A., Shahidan, S., Rahman, R.A., 2017. A review on seashells ash as partial cement replacement. IOP Conf. Ser. Mater. Sci. Eng. 271, 12059.

[Motamedi et al. 2015] Motamedi, S., Shamshirband, S., Hashim, R., Petković, D., Roy, C., 2015. Estimating unconfined compressive strength of cockle shell-cement-sand mixtures using soft computing methodologies. Eng. Struct. 98, 49–58.

[Nazari and Ghafouri 2013] Nazari, A., Ghafouri Safarnejad, M., 2013. Prediction early age compressive strength of OPC-based geopolymers with different alkali activators and seashell powder by gene expression programming. Ceram. Int. 39, 1433–1442.

[Piasta and Sikora 2015] Piasta, W., Sikora, H., 2015. Effect of air entrainment on shrinkage of blended cements concretes. Constr. Build. Mater. 99, 298–307.

[Rashed and Williamson 1991] Rashed, A.I., Williamson, R.B., 1991. Microstructure of entrained air voids in concrete, Part I. J. Mater. Res. 6, 2004–2012.

[Safi et al 2015] Safi, B., Saidi, M., Daoui, A., Bellal, A., Mechekak, A., Toumi, K., 2015. The use of seashells as a fine aggregate (by sand substitution) in self-compacting mortar (SCM). Constr. Build. Mater. 78, 430–438.

[Silva et al 2016] Silva, R. V., De Brito, J., Dhir, R.K., 2016. Performance of cementitious renderings and masonry mortars containing recycled aggregates from construction and demolition wastes. Constr. Build. Mater. 105, 400–415

[Topçu et al. 2017] Topçu, İ., Ateşin, Ö., Uygunoğlu, T., 2017. Effect of High Dosage Air-Entraining Admixture Usage on Micro Concrete Properties, European Journal of Engineering and Natural Sciences (EJENS).

[Wang et al. 2013] Wang, H.Y., Kuo, W. Ten, Lin, C.C., Po-Yo, C., 2013. Study of the material properties of fly ash added to oyster cement mortar. Constr. Build. Mater. 41, 532–537.

[Wong et al 2011] Wong, H.S., Pappas, A.M., Zimmerman, R.W., Buenfeld, N.R., 2011. Effect of entrained air voids on the microstructure and mass transport properties of concrete. Cem. Concr. Res. 41, 1067–1077.

[Yoon et al 2003] Yoon, G., Kim, B., Kim, B., Han, S., 2003. Chemical – mechanical characteristics of crushed oyster-shell. Waste Manag. 23, 825–834.

[Yoon 2004] Yoon, H., 2004. Oyster Shell as Substitute for Aggregate in Mortar. Waste Manag. Res. 22, 158–170.